Optimal statistical design of variable sample size multivariate exponentially weighted moving average control chart based on median run-length

Optimal Statistical Design of Variable Sample Size Multivariate Exponentially Weighted Moving Average Control Chart Based on Median Run-Length

Siow Yin Nyau[*a], Ming Ha Lee[a], M. L. Dennis Wong[b]

[a]*Faculty of Engineering, Computing and Science, Swinburne University of Technology Sarawak Campus, Kuching, Malaysia;*

[b]*Heriot-Watt University Malaysia, Putrajaya, Malaysia*

[*]Email: snyau@swinburne.edu.my

Nyau Siow Yin, is a PhD Student from the Faculty of Engineering, Computing and Science, Swinburne University of Technology Sarawak Campus, Malaysia. She holds a Bachelor of Engineering in Mechanical Engineering from the same university. Her research interest is in statistical process control.

Ming Ha Lee, is a Senior Lecturer in the Faculty of Engineering, Computing and Science, Swinburne University of Technology Sarawak Campus, Malaysia. She obtained her PhD in Statistics from the Universiti Sains Malaysia. Her current research interest is statistical process control.

M.L. Dennis Wong, is a Professor at Heriot-Watt University Malaysia. He received his BEng (Hons) and PhD from the Department of Electrical Engineering and Electronics, University of Liverpool, Liverpool, UK. His current research interests include statistical pattern classification, machine condition monitoring, and biometrics template protection.

Optimal Statistical Design of Variable Sample Size Multivariate Exponentially Weighted Moving Average Control Chart Based on Median Run-Length

Conventionally, a standard control chart implements fixed sample size in process monitoring. In this study, we propose an optimal statistical design for the variable sample size (VSS) multivariate exponentially weighted moving average (MEWMA) chart based on the median run-length (*MRL*). The proposal is based on the fact that the percentiles of the run-length distribution, especially the *MRL*, are more reflective and reliable for performance evaluation with respect to a skewed run-length distribution. The *MRL* for the VSS MEWMA chart computed using the Markov chain approach is verified with Monte Carlo simulation. For benchmarking purposes, the performance of the VSS MEWMA chart is compared against the standard MEWMA chart and the synthetic T^2 chart, in terms of the *MRL*. The numerical results show that the VSS MEWMA chart performs better than the standard MEWMA chart and the synthetic T^2 chart, in detecting shifts in the process mean vector. Finally, an application is provided as an illustration for the implementation of the VSS MEWMA chart based on the *MRL*.

Keywords: Markov chain approach; median run-length; multivariate exponentially weighted moving average chart; variable sample size

1. Introduction

A control chart illustrates the state of a process over time to detect and minimize variability in the process monitoring. Recently, considerable efforts have been undertaken on the research of various multivariate control charts since the quality of a product is usually affected by multiple characteristics of the product (Qiu, 2013). Bersimis, Psarakis, and Panaretos (2007); and Lowry and Montgomery (1995) reviewed the procedures for the implementation of the multivariate control charts. For literature on the multivariate control charts, refer to Chen, Zi, and Zou (2016); Cheng and Mao (2011); Das (2009); Ghute and Shirke (2008b); Lee (2013); Li, Tsung, and Zou (2014); Maboudou-Tchao and Diawara (2013); Reynolds and Cho (2011); Seif, Faraz, and Sadeghifar (2015); Zi, Zou, Zhou, and Wang (2013); and Zou and Tsung (2011).

The variable sample size (VSS) scheme is one of the methods used to improve the efficiency of control charts, whereby the sample size can be varied according to the plotted statistics on the chart. According to Lee (2010), the multivariate exponentially weighted moving average (MEWMA) chart with the VSS scheme is proven to be more effective than the standard MEWMA chart for monitoring the process mean vector, in terms of the average run-length (*ARL*). Hence, the VSS scheme is adopted in this study to statistically improve the performance of the MEWMA chart. Besides, this study complements the work by Lee (2010) by using the median run-length (*MRL*) as a performance measure. As such, the main objective of this study is to design an optimal VSS MEWMA chart based on the *MRL* for monitoring the process mean vector.

The outline of the rest of this article is as follows: Section 2 briefly reviews the *MRL*, the MEWMA chart and the VSS scheme. Section 3 discusses the properties of the VSS MEWMA chart. In Section 4, the Markov chain approach described in Runger and Prabhu (1996) is modified to evaluate the performance of the VSS MEWMA chart

based on the *MRL* for both zero-state and steady-state cases. Section 5 highlights the optimal statistical design of the VSS MEWMA chart based on the *MRL*. The run-length distribution is illustrated in Section 6 for a better understanding of the VSS MEWMA chart. A detailed comparative study is presented in Section 7. An illustrative example is given in Section 8 to demonstrate the application of the VSS MEWMA chart. Finally, Section 9 summarizes the main findings and concludes the paper.

2. Literature Review

This section briefly reviews the major concepts of this study. These include the *MRL*, the MEWMA chart and the VSS scheme to better understand this study.

2.1 MRL

The common performance measure of a control chart is the *ARL*. However, the sole reliance on the *ARL* has been subject to criticism in recent years (Montgomery, 2013). As pointed out by Gan (1993); Golosnoy and Schmid (2007); and Palm (1990), the run-length distribution is highly skewed when the process is in control and nearly symmetrical at a larger shift. Therefore, the conclusion based on the *ARL* can be misleading as it is not necessarily a typical run-length.

The works of Dyer, Adams, and Conerly (2003) and Maravelakis, Panaretos, and Psarakis (2005) confirmed that the *MRL* is a more credible performance measure for a control chart as it is less affected by the skewness of the run-length distribution. In addition, more researchers such as Chakraborti (2007); Chin and Khoo (2012); Graham, Mukherjee, and Chakraborti (2012); Khoo, Teh, Chuah, and Foo (2011); Khoo, Wong, Wu, and Castagliola (2012); Khoo, Wong, Wu, and Castagliola (2011); Low, Khoo, Teoh, and Wu (2012); Mukherjee and Marozzi (2016b); and Teoh, Khoo, and Teh (2013) advocated using the *MRL* as an alternative measure for their proposed control

charts. Following these researchers, this study proposes to make use of the *MRL* as the performance measure.

2.2 MEWMA Chart

The MEWMA chart was introduced by Lowry, Woodall, Champ, and Rigdon (1992) as an extension of the univariate exponentially weighted moving average chart. Runger and Prabhu (1996) applied the Markov chain approach to evaluate the performance of the MEWMA chart based on the *ARL*. Molnau et al. (2001) presented a computer program for computing the *ARL* values of the MEWMA chart. For the recent developments in the design of the MEWMA chart, see Aly, Mahmoud, and Hamed (2016); Mahmoud and Maravelakis (2010); Mahmoud and Zahran (2010); Park and Jun (2015); and Shen, Tsung, and Zou (2014).

2.3 VSS Scheme

The VSS scheme is implemented in such a way that a large sample size will be used if there is an indication of a possible variation in the process; whereas a small sample size will be used if there is no such indication. It is known that the VSS scheme improves the statistical efficiency of control charts in detecting process shifts. Therefore, the VSS scheme has been studied extensively among researchers. For example, see Aparisi (1996); Aparisi, Epprecht, Carrión, and Ruiz (2014); Castagliola, Achouri, Taleb, Celano, and Psarakis (2015); Castagliola, Zhang, Costa, and Maravelakis (2012); Faraz and Moghadam (2009); Huang, Shu, Woodall, and Tsui (2016); Kooli and Limam (2011); and Prabhu, Runger, and Montgomery (1997).

3. Properties of the VSS MEWMA Chart

Let X_{vkt} denote observation v for quality characteristic k at sampling point t, where $v = 1$,

2, 3, …, n; k = 1, 2, 3, …, p and t = 1, 2, 3, …. It is assumed that the process is normally distributed with independent and identical observations. The sample mean for the quality characteristic k at the sampling point t is given as

$$\overline{X}_{kt} = \frac{\sum_{v=1}^{n} X_{vkt}}{n}. \tag{1}$$

Then, the sample mean vector at the sampling point t is $\tilde{\overline{\mathbf{X}}}_t = (\overline{X}_{1t}, \overline{X}_{2t}, \overline{X}_{3t}, \ldots, \overline{X}_{pt})^T$. It is assumed that $\tilde{\overline{\mathbf{X}}}_t$ has a multivariate normal distribution with mean vector $\tilde{\boldsymbol{\mu}} = (\mu_1, \mu_2, \ldots, \mu_p)^T$ and $p \times p$ covariance matrix $\tilde{\boldsymbol{\Sigma}}$. The standardized sample mean for the quality characteristic k at the sampling point t is

$$Z_{kt} = \frac{\overline{X}_{kt} - \mu_{0k}}{\frac{\sigma_{0k}}{\sqrt{n}}}, \tag{2}$$

where μ_{0k} is the kth component of the in-control process mean vector $\tilde{\boldsymbol{\mu}}_0$ and σ_{0k} is the kth component of the in-control process standard deviation vector $\tilde{\boldsymbol{\sigma}}_0$. The standardized sample mean vector at the sampling point t is given as $\tilde{\mathbf{Z}}_t = (Z_{1t}, Z_{2t}, Z_{3t}, \ldots, Z_{pt})^T$, then $\tilde{\mathbf{Z}}_1, \tilde{\mathbf{Z}}_2, \tilde{\mathbf{Z}}_3, \ldots$ are vectors with p components. The MEWMA vector proposed by Lowry et al. (1992) is defined as

$$\tilde{\mathbf{W}}_t = r\tilde{\mathbf{Z}}_t + (1-r)\tilde{\mathbf{W}}_{t-1}, \tag{3}$$

for t = 1, 2, 3, …, where $\tilde{\mathbf{W}}_0 = \tilde{\mathbf{0}}$ and $0 < r \leq 1$ is the smoothing constant. Hence, the MEWMA chart has the plotted chart statistics

$$T_t^2 = \mathbf{W}_t^T \, \tilde{\tilde{\Sigma}}_{\mathbf{W}}^{-1} \, \tilde{\mathbf{W}}_t , \qquad (4)$$

for t = 1, 2, 3, …, where $\tilde{\tilde{\Sigma}}_{\mathbf{W}}$ is the covariance matrix of $\tilde{\mathbf{W}}_t$. In this study, the asymptotic covariance matrix $\tilde{\tilde{\Sigma}}_{\mathbf{W}} = \left(\frac{r}{2-r} \right) \tilde{\tilde{\Sigma}}_{\mathbf{Z}}$ is used, where $\tilde{\tilde{\Sigma}}_{\mathbf{Z}}$ is the correlation matrix of $\tilde{\mathbf{Z}}_t$. Note that $\tilde{\tilde{\Sigma}}_{\mathbf{Z}}$ is the covariance matrix $\tilde{\tilde{\Sigma}}$ in correlation form. An out-of-control signal is triggered when $T_t^2 > H$, where $H > 0$ is the control limit. The control limit H is chosen to provide a specific value for the in-control performance measure.

Lowry et al. (1992) showed that the MEWMA chart is directionally invariant. In other words, they showed that the *ARL* performance of the MEWMA chart is determined solely by the distance of the out-of-control process mean vector $\tilde{\boldsymbol{\mu}} = \tilde{\boldsymbol{\mu}}_1$ from the in-control process mean vector $\tilde{\boldsymbol{\mu}} = \tilde{\boldsymbol{\mu}}_0$. This distance is defined as the square root of the non-centrality parameter, which is the size of a shift $\delta = \sqrt{\tilde{\mathbf{v}}^T \, \tilde{\tilde{\Sigma}}_{\mathbf{Z}}^{-1} \, \tilde{\mathbf{v}}}$, where $\tilde{\mathbf{v}}$ is the standardized mean vector. Here, the kth component of $\tilde{\mathbf{v}}$ is $v_k = (\mu_k - \mu_{0k})/\sigma_{0k}$, where μ_{0k} is the kth component of the in-control process mean vector $\tilde{\boldsymbol{\mu}}_0$ and σ_{0k} is the kth component of the in-control process standard deviation vector $\tilde{\boldsymbol{\sigma}}_0$. Because of the directional invariance property of the MEWMA chart, the value of the performance measure is the same for any out-of-control process mean vectors that have the same distance from the in-control process mean vector. It is assumed that $\tilde{\tilde{\Sigma}}_{\mathbf{Z}}$ is an in-control process correlation matrix since $\tilde{\tilde{\Sigma}}_{\mathbf{Z}}$ remains constant.

For the standard MEWMA chart, the sample size is being fixed as n_0; whereas for the VSS MEWMA chart, a warning limit w is introduced, such that $0 < w < H$. The value of w acts as an indicator for the change in the sample size, such that $n_1 < n_0 < n_2$,

where n_1 is the small sample size and n_2 is the large sample size. The values of n_1 and n_2 in the VSS MEWMA chart are chosen in order to obtain an average sample size $E(n) = n_0$. This two-sample size chart consists of three regions which are the safety, warning and action regions. The function of the two-state VSS MEWMA chart is defined as

$$n = \begin{cases} n_1 & \text{if } T_t^2 \le w \\ n_2 & \text{if } w < T_t^2 \le H \end{cases}.$$

If the current sample falls inside the safety region ($T_t^2 \le w$), a sample of size n_1 will be taken at the next sampling point; whereas if the current sample falls inside the warning region ($w < T_t^2 \le H$), a sample of size n_2 will be taken at the next sampling point. An out-of-control signal will be triggered if the current sample falls inside the action region ($T_t^2 > H$). When the process is just starting or after a false alarm, the first sample size can be chosen at random. Alternatively, it may be preferable to use tightening control, which is the large sample of size n_2 as it provides an extra protection against problems that may arise during start-up. The operation procedure of the VSS MEWMA chart is as follows:

(1) Take a sample of size n_2.

(2) Calculate the plotted chart statistic T_t^2.

(3) The current sample position of T_t^2 determines the size of the sample at the next sampling point such that:

a. if the current sample falls inside the safety region ($T_t^2 \le w$), a sample of size n_1 will be taken at the next sampling point since there is no apparent risk in the process and the control flows back to Step 2.

b. if the current sample falls inside the warning region ($w < T_t^2 \leq H$), a sample of size n_2 will be taken at the next sampling point and the control flows back to Step 2.

For these two cases, the sample is considered as conforming. Otherwise, the sample is considered to be nonconforming and the control flows to the next step.

(4) The current sample falls inside the action region ($T_t^2 > H$), an out-of-control signal would be triggered. Search and eliminate the assignable cause(s). Then, the control flows back to Step 1.

4. Markov Chain Approach

Runger and Prabhu (1996) developed a Markov chain approach to calculate the *ARL* of the MEWMA chart. In this study, the Markov chain approach of Runger and Prabhu (1996) is modified to evaluate the performance of the VSS MEWMA chart based on the *MRL*. Let $T_t^2 = b\left\|\tilde{\mathbf{W}}_t\right\|$, where $b = (2 - r)/r$ and the statistic $q_t = \left\|\tilde{\mathbf{W}}_t\right\|$ is plotted with q_t being a measure of distance in p-dimensional space, then UCL = $\sqrt{H/b}$ and UWL = $\sqrt{w/b}$. Runger and Prabhu (1996) have shown that the out-of-control *ARL* (ARL_1) of the standard MEWMA chart with the fixed sample size can be analyzed by using a two-dimensional Markov chain, in which $\tilde{\mathbf{W}}_t$ is partitioned into W_{t1} and $\left\|\tilde{\mathbf{W}}_{t2}\right\|$. In this study, modifications are necessary to obtain the *MRL* of the VSS MEWMA chart. The horizontal transition probability of W_{t1} is used to analyze the out-of-control component. Let m be the number of states of the Markov chain, then the horizontal transition probability of W_{t1} from state i_x to state j_x is denoted by

$$h(i_x, j_x) = \Phi\left[\frac{-\text{UCL} + j_x g - (1-r)c_{i_x}}{r} - \delta\sqrt{n}\right] - \Phi\left[\frac{-\text{UCL} + (j_x - 1)g - (1-r)c_{i_x}}{r} - \delta\sqrt{n}\right], \quad (5)$$

for i_x, j_x = 1, 2, ..., 2m + 1, where $\Phi(\cdot)$ represents the cumulative probability distribution function of a standard normal random variable with c_{i_x} = –UCL + (i_x – 0.5)g be the centerpoint of state i_x; g = 2UCL/(2m + 1) is the width of each state and n is the sample size.

The vertical transition probability of $\left\|\tilde{\mathbf{W}}_{t2}\right\|$ is used to analyze the in-control component. For i_y = 0, 1, 2, …, m and j_y = 1, 2, …, m, the vertical transition probability of $\left\|\tilde{\mathbf{W}}_{t2}\right\|$ from state i_y to state j_y is denoted by

$$v(i_y, j_y) = \Pr\left[\frac{(j_y - 0.5)^2 g^2}{r^2} < \chi^2(p-1, c) < \frac{(j_y + 0.5)^2 g^2}{r^2}\right], \quad (6)$$

where $\chi^2(p - 1, c)$ is a non-central chi-square random variable with (p – 1) degrees of freedom and non-centrality parameter $c = \left[(1-r)i_y g / r\right]^2$. For j_y = 0,

$$v(i_y, 0) = \Pr\left[\chi^2(p-1, c) < \frac{0.5^2 g^2}{r^2}\right]. \quad (7)$$

The transition probability of the bivariate model from state (i_x, i_y) to state (j_x, j_y) is Pr[(i_x, i_y), (j_x, j_y)] = $h(i_x, j_x)v(i_y, j_y)$ and the value of n in Equation (5) is given as

$$n = \begin{cases} n_1 & \text{if } [i_x - (m+1)]^2 g^2 + i_y^2 g^2 \le \text{UWL}^2 \\ n_2 & \text{if } \text{UWL}^2 < [i_x - (m+1)]^2 g^2 + i_y^2 g^2 \le \text{UCL}^2 \\ 0 & \text{otherwise} \end{cases}, \quad (8)$$

where $n = n_1$ if state (i_x, i_y) falls inside the safety region ($T_t^2 \le w$) and $n = n_2$ if state (i_x, i_y) falls inside the warning region ($w < T_t^2 \le H$). Then, $\tilde{\mathbf{n}}$ = {(1, 0), (1, 1), (1, 2), (1, 3), …, (1, m), (2, 0), (2, 1), (2, 2), (2, 3), …, (2, m), (3, 0), (3, 1), (3, 2), (3, 3), …, (3, m), …, ($2m$ + 1, 0), ($2m$ + 1, 1), ($2m$ + 1, 2), …, ($2m$ + 1, m)}^{T}, is a ($2m$ + 1)(m + 1) vector. When $n_1 = n_2 = n_0$ and $H = w$, the VSS MEWMA chart becomes the standard MEWMA chart. Interested readers are referred to Runger and Prabhu (1996) for more details on the horizontal and vertical transition probabilities.

Let $\tilde{\mathbf{Q}}$ denote the ($2m$ + 1)(m + 1) × ($2m$ + 1)(m + 1) transition probability matrix of the two-dimensional Markov chain. Then $\tilde{\mathbf{Q}} = \tilde{\mathbf{H}} \otimes \tilde{\mathbf{V}}$, where ⊗ is the Kronecker product of the matrices, $\tilde{\mathbf{H}}$ is the horizontal transition probability matrix and $\tilde{\mathbf{V}}$ is the vertical transition probability matrix. Let $\tilde{\mathbf{T}}$ denote a ($2m$ + 1)(m + 1) × ($2m$ + 1)(m + 1) matrix with

$$\tilde{\mathbf{T}}(i_x, i_y) = \begin{cases} 1 & \text{if state}(i_x, i_y) \text{ is a transient state} \\ 0 & \text{if state}(i_x, i_y) \text{ is an absorbing state} \end{cases}. \qquad (9)$$

Let $\tilde{\mathbf{Q}}_t$ be the transition probability matrix that contains the transient states of the bivariate Markov chain, then $\tilde{\mathbf{Q}}_t = \tilde{\mathbf{T}} \; \Theta \; \tilde{\mathbf{Q}}$, where Θ denotes the element-wise multiplication of the matrices.

In this study, the Markov chain with the number of states m = 25 is used to compute the performance measures of the VSS MEWMA chart. For a detailed explanation on the number of states for the Markov chain, refer to Molnau et al. (2001). Let R be the run-length of a control chart, then the zero-state cumulative run-length probability is computed as (Brook & Evans, 1972)

$$\Pr(R \le r) = \tilde{\mathbf{s}}^T (\tilde{\mathbf{I}} - \tilde{\mathbf{Q}}_t^r)\tilde{\mathbf{1}}, \tag{10}$$

for r = 1, 2, 3, …, where $\tilde{\mathbf{Q}}_t$ contains the transition probabilities of all the transient states in the Markov chain; $\tilde{\mathbf{s}}$ is the (2m + 1)(m + 1) initial probability vector with a 1 in the [m(m + 1) + 1]th element corresponding to the starting state of the Markov chain and zeros elsewhere; $\tilde{\mathbf{I}}$ is the (2m + 1)(m + 1) dimensional identity matrix and $\tilde{\mathbf{1}}$ is a (2m + 1)(m + 1) vector with unit entries. The zero-state run-length probability for a control chart is defined by Brook and Evans (1972) as

$$\Pr(R = r) = \tilde{\mathbf{s}}^T \tilde{\mathbf{Q}}_t^{r-1} (\tilde{\mathbf{I}} - \tilde{\mathbf{Q}}_t)\tilde{\mathbf{1}}. \tag{11}$$

For the steady-state case, the initial probability vector $\tilde{\mathbf{s}}$ in Equations (10) and (11) is replaced with the steady-state probability vector

$$\tilde{\mathbf{s}}_0 = (\tilde{\mathbf{1}}^T \tilde{\mathbf{q}})^{-1} \tilde{\mathbf{q}}, \tag{12}$$

as proposed by Champ (1992). Here, $\tilde{\mathbf{q}} = \left(\tilde{\mathbf{G}} - \tilde{\mathbf{Q}}_0^T\right)^{-1} \tilde{\mathbf{u}}$, where

$$\tilde{\mathbf{G}} = \begin{pmatrix} 2 & 1 & 1 & \cdots & 1 \\ 0 & 1 & 0 & \cdots & 0 \\ 0 & 0 & 1 & \cdots & 0 \\ \vdots & \vdots & \vdots & \ddots & \vdots \\ 0 & 0 & 0 & \cdots & 1 \end{pmatrix}$$

is a (2m + 1)(m + 1) × (2m + 1)(m + 1) matrix; $\tilde{\mathbf{Q}}_0$ is constructed by dividing each element of $\tilde{\mathbf{Q}}_t$ by the sum of its row with δ = 0 and $\tilde{\mathbf{u}}$ = (1, 0, 0, …, 0)^T. Then, the steady-state cumulative run-length probability is computed as

$$\Pr(R \le r) = \tilde{\mathbf{s}}_0^T (\tilde{\mathbf{I}} - \tilde{\mathbf{Q}}_t^r)\tilde{\mathbf{1}}. \tag{13}$$

Gan(1993) showed that the 100γth percentile can be calculated as

$$\Pr(R \le r-1) \le \gamma \text{ and } \Pr(R \le r) > \gamma \ . \tag{14}$$

The *MRL* of the VSS MEWMA chart can be computed by using γ = 0.5 in Equation (14). The zero-state *MRL* is used when the process mean vector shifts off-target ($\tilde{\boldsymbol{\mu}}$ = $\tilde{\boldsymbol{\mu}}_1$) at the beginning of the process monitoring. On the other hand, the steady-state case assumes that the process mean vector is initially on-target ($\tilde{\boldsymbol{\mu}}$ = $\tilde{\boldsymbol{\mu}}_0$) and the process stays in control for a period of time before the process mean vector shifts off-target ($\tilde{\boldsymbol{\mu}}$ = $\tilde{\boldsymbol{\mu}}_1$) at some random time in the future (Stoumbos, Mittenthal, & Runger, 2001). Here, the steady-state performance is considered as the time from the shift in the process mean vector until a signal. In most practical situations, the process usually starts in control and an assignable cause shifts the process mean vector at some random time in the future. Hence, the steady-state performance is generally more important than the zero-state performance when $\delta \neq 0$ (Haq & Khoo, 2016; Mukerjee & Marozzi, 2016a).

The zero-state in-control average run-length and the zero-state in-control average number of observations to signal for the VSS MEWMA chart (Lee, 2010) are

$$ARL_0 = \tilde{\mathbf{s}}^T (\tilde{\mathbf{I}} - \tilde{\mathbf{Q}}_t)^{-1} \tilde{\mathbf{1}} \tag{15}$$

and

$$ANOS_0 = \tilde{\mathbf{s}}^T (\tilde{\mathbf{I}} - \tilde{\mathbf{Q}}_t)^{-1} \tilde{\mathbf{n}}, \tag{16}$$

respectively, where δ = 0. Then, the in-control average sample size of the VSS MEWMA chart (Lee, 2010) is given as

$$E(n) = \frac{ANOS_0}{ARL_0}. \quad (17)$$

5. Optimal Design of the VSS MEWMA Chart

In this study, the optimal statistical design of the VSS MEWMA chart is proposed by minimizing the out-of-control *MRL* (MRL_1). This involves the computation of the following optimal charting parameters: (i) r: the smoothing constant, (ii) n_1: the small sample size, (iii) n_2: the large sample size, (iv) H: the control limit and (v) w: the warning limit. In developing the optimal statistical design, the following decision variables are considered: (i) p: the number of quality characteristics, (ii) MRL_0: the desired in-control *MRL*, (iii) $E(n)$: the in-control average sample size and (iv) δ_{opt}: the shift in the process mean vector. Note that δ_{opt} is the magnitude of shift in the process mean vector for which a quick detection is required.

The MRL_0 of a control chart should be large enough to minimize the false alarm rate. Conversely, the MRL_1 should be small, indicating a control chart that quickly detects shifts in the process mean vector. Referring to Graham, Chakraborti, and Mukherjee (2014), $ARL_0 \approx 500$ is used as the industry standard value and it corresponds to $MRL_0 \approx 350$. Hence, $MRL_0 = 350$ is chosen as the nominal target in this study.

Some constraints are considered for the optimal design of the VSS MEWMA chart based on the *MRL*. For the VSS MEWMA chart, only two sample sizes are used, i.e. n_1 and n_2. The small sample size is set to be $n_1 = 1, 2, \ldots, n_0 - 1$ and the large sample size is set to be $n_2 = n_0 + 1, n_0 + 2, ..., 20$, where $n_1 < n_0 < n_2$. Here, $E(n) = n_0$. Following Faraz and Moghadam (2009), the largest sample size is set as 20 because it is not realistic to have a large number of the sample size to be examined during the process quality control. In addition, Castagliola et al. (2012) stated that it is more

practical to have small and moderate sample sizes in industries. More importantly, the value of the large sample size was found to be optimized before it reaches $n_2 = 20$.

An exhaustive search algorithm is used to determine the optimal charting parameters (r, n_1, n_2, H, w) for the VSS MEWMA chart. The procedure for the optimal statistical design of the VSS MEWMA chart based on the *MRL* is outlined below:

(1) Specify the values of MRL_0, $E(n)$, p and δ_{opt}.

(2) Initialize $r = 0.005$.

(3) Given the r value in Step 2, set the shift as $\delta = 0$, compute the control limit H for the specified MRL_0, using Equation (14) with $\gamma = 0.5$.

(4) For each value of $n_1 = 1, 2, \ldots, n_0 - 1$, compute the warning limit w for the specified MRL_0 with the values of $n_2 = n_0 + 1, n_0 + 2, ..., 20$ to obtain $E(n) = n_0$, using Equation (17). Note that $w < H$.

(5) Compute the MRL_1 at the specified δ_{opt} using Equation (14) with $\gamma = 0.5$.

(6) Repeat Steps 3 to 5 for the values of r from 0.01 to 0.10 with step size 0.005 and then for the values of r from 0.11 to 1.00 with step size 0.01.

(7) The combination of charting parameters (r, n_1, n_2, H, w) that produces the minimum MRL_1 is recorded as the optimal charting parameters of the VSS MEWMA chart.

Since the *MRL* is a distinct quantity, there can be a few combinations of the optimal charting parameters that will produce the same minimum value of MRL_1 for an interval of the smoothing constant r at a particular δ_{opt}. Here, the center value for the range of the optimal r that produces the same minimum MRL_1 is selected as the optimal value of r.

6. Run-length Distribution of the VSS MEWMA chart

Using the procedure of the optimal statistical design described in the previous section, the optimal charting parameters of the VSS MEWMA chart based on the zero-state case for $E(n) = 5$, $MRL_0 = 350$ and $p = 3$ at $\delta_{opt} = 0.50$ are obtained as $(r, n_1, n_2, H, w) = (0.30, 4, 13, 14.401, 5.869)$. The plots of the run-length probability distribution for this VSS MEWMA chart for $\delta = 0.00, 0.25, 0.50, 1.00, 2.00$ and 2.50 are given in Figure 1. Here, the run-length probabilities are calculated using Equation (11). Figure 1 shows that the run-length distribution of the VSS MEWMA chart is highly skewed when the process is in control ($\delta = 0$) or slightly out of control ($\delta = 0.25$); whereas at a larger shift, for example, when $\delta = 1.00$, the run-length distribution is almost symmetric. The changes in the shape of the run-length distribution according to the magnitude of shifts in the process mean vector clearly demonstrate that the run-length distribution for the VSS MEWMA chart is highly skewed to the right (positively skewed) when the process is in control to nearly symmetrical at the larger shifts.

The interpretation based on the *ARL* with respect to a skewed run-length distribution would certainly be different from that based on the *ARL* with respect to an almost symmetric distribution. Thus, the interpretation based on the *ARL* can be confusing when the run-length distribution changes with the shift. On the other hand, the use of the *MRL* is more readily comprehensible in providing information on the performance of a control chart with respect to the skewed run-length distribution.

Table 1 firstly provides the percentage points of the run-length for the steady-state VSS MEWMA chart with $p = 2$ at $\delta_{opt} \in \{0.50, 1.00\}$ for $E(n) = 5$ and $ARL_0 \approx 500$. The 1st, 5th, 10th, 20th, 30th, 40th, 50th, 60th, 70th, 80th and 90th percentage points (or percentiles) of the run-length distribution are computed using Equation (14). Note that the 50th percentile is the *MRL*. It is observed that the ARL_1s are larger than the

corresponding MRL_1s for all the given δ_{opt} due to the skewed run-length distribution. For example, when δ_{opt} = 0.50, p = 2 and $E(n)$ = 5 are considered, ARL_1 = 32.61 but MRL_1 = 24 at δ = 0.25 for the VSS MEWMA chart with the optimal charting parameters (r, n_1, n_2, H, w) = (0.43, 1, 21, 12.228, 3.197). This shows that using the *ARL* as a performance measure for the control chart can be confusing and misleading as the average does not represent "half the time" (Palm, 1990).

Secondly, Table 1 shows that the difference between the ARL_1 and MRL_1 decreases as the shift δ increases. The values of ARL_1 and MRL_1 are similar with a negligible difference ($|ARL_1 - MRL_1| \leq 1.00$) at $\delta \geq 1.50$. For example, at δ = 2.00, the VSS MEWMA chart with the optimal charting parameters (r, n_1, n_2, H, w) = (0.43, 1, 21, 12.228, 3.197) gives ARL_1 = 2.19 and MRL_1 = 2, where $|ARL_1 - MRL_1|$ = 0.19. However, at a smaller shift, such as δ = 0.25, the chart gives ARL_1 = 32.61 and MRL_1 = 24, where $|ARL_1 - MRL_1|$ = 8.61.

Thirdly, Table 1 also provides information such as the early false alarm rates. The early false alarm rates can be obtained from the smaller percentage points, such as 1st, 5th and 10th percentiles of the run-length distribution under δ = 0. For example, although the ARL_0 of the VSS MEWMA chart with (r, n_1, n_2, H, w) = (0.43, 1, 21, 12.228, 3.197) is given as 498.33, there is a 5% chance that a false alarm will be observed by the 26th sample.

Fourthly, Table 1 provides the higher percentage points of the run-length, in which a higher percentage point shows that an out-of-control signal will be triggered with a higher probability when the process shifts by a certain magnitude. For example, the VSS MEWMA chart with (r, n_1, n_2, H, w) = (0.43, 1, 21, 12.228, 3.197), there is a 90% chance that an out-of-control signal will be detected by the 71st sample for δ =

0.25. In other words, this control chart signals within the first 71 samples with the probability of 0.9.

In addition, Table 1 shows that the MRL_0 value of the VSS MEWMA chart is less than the corresponding ARL_0 value. For example, for the VSS MEWMA chart with $(r, n_1, n_2, H, w) = (0.43, 1, 21, 12.228, 3.197)$, the MRL_0 is 346 while the ARL_0 is 498.33. Based on the entire run-length distribution, the ARL_0 lies between the 60th and 70th percentiles of the run-length distribution. This means that the in-control run-length distribution is skewed to the right. The MRL_0 of 346 indicates that a false alarm will be observed by the 346th sample in half the time.

From these results, it can be concluded that the percentiles of the run-length distribution provide a more meaningful interpretation for the in-control and out-of-control performances of the VSS MEWMA chart. Furthermore, the percentiles of the run-length distribution provide practitioners with a more comprehensive understanding of the behaviour of the VSS MEWMA chart.

7. Performance Comparison between the Control Charts based on the *MRL*

In this study, the performance of the VSS MEWMA chart is compared with the standard MEWMA chart and the synthetic T^2 chart based on the *MRL*. A brief review of the competing charts is provided in the following sub-sections.

7.1 Standard MEWMA chart

Lowry et al. (1992) presented the standard MEWMA chart where the statistical design involves the selection of the optimal charting parameters: (i) r: the smoothing constant and (ii) H: the control limit for which the sample size is fixed as n_0. For a detailed discussion for the optimal statistical design of the standard MEWMA chart based on the

MRL, refer to Lee and Khoo (2006).

7.2 Synthetic T^2 Chart

The synthetic T^2 chart is a combination of the Hotelling's T^2 chart and the conforming run-length chart for monitoring the mean of a multivariate normal distribution process (Ghute & Shirke, 2008a). The statistical design of the synthetic T^2 chart involves the selection of the optimal charting parameters: (i) L: the lower control limit and (ii) CL: the upper control limit.

7.3 Performance Comparison between the Control Charts

Table 2 presents the optimal charting parameters for the VSS MEWMA chart, the standard MEWMA chart and the synthetic T^2 chart. For comparison purposes, the optimal charting parameters are obtained for shifts at $\delta_{opt} \in \{0.25, 0.50, 1.00, 1.50, 2.00, 2.50\}$ with $E(n) = 5$, $MRL_0 = 350$ and $p \in \{2, 3, 5\}$, where the MRL_1 is minimized at each δ_{opt}. The MRL_1s for all the optimized charts are provided in Table 3. Note that the optimal charting parameters and the corresponding MRL_1 of the synthetic T^2 chart are obtained by adopting the methodology in Khoo et al. (2011). The MRL_0 of 350 indicates that a false alarm will be observed, within the first 350 samples, at least 50% of the time. When $\delta_{opt} \neq 0$, for example, at $\delta_{opt} = 0.25$ for $p = 2$, a zero-state MRL_1 of 17 for the VSS MEWMA chart (see Table 3) indicating there is a 50% chance that an out-of-control signal will be triggered by the 17th sample.

Table 3 shows that for the zero-state case, the VSS MEWMA chart outperforms the standard MEWMA chart and the synthetic T^2 chart for $\delta_{opt} \leq 0.50$; the synthetic T^2 chart only performs slightly better than the VSS MEWMA chart or the standard MEWMA chart for $1.00 \leq \delta_{opt} \leq 1.50$, the performance of the VSS MEWMA chart is the same as that of the standard MEWMA chart and the synthetic T^2 chart for $\delta_{opt} \geq 2.00$

since all the control charts give the same MRL_1 values. For the steady-state case, the VSS MEWMA chart performs consistently better or at least on a par with the standard MEWMA chart and synthetic T^2 chart in detecting small shifts ($\delta_{opt} \leq 1.50$), where all the MRL_1 values of the VSS MEWMA chart are smaller than or equal to the standard MEWMA chart and the synthetic T^2 chart. The performance of the VSS MEWMA chart or the standard MEWMA chart is slightly better than the synthetic T^2 chart for $\delta_{opt} \geq 2.00$. From these results, it can be concluded that the VSS MEWMA chart performs better than the standard MEWMA chart and the synthetic T^2 chart, especially for the steady-state case.

Table 4 gives the quartile deviation of the run-length distribution (*QDRL*) for each of the optimized chart shown in Table 3. The *QDRL* defined as one-half the difference between the first and third quartiles is computed to demonstrate the variability in the run-length distribution. The *QDRL* can be presented as:

$$QDRL = \frac{Q3 - Q1}{2}, \tag{18}$$

where $Q1$ and $Q3$ are the 25th and 75th percentiles of the run-length distribution, respectively. Table 4 shows that the run-length distribution of the VSS MEWMA chart has a smaller variability than that of the standard MEWMA chart and the synthetic T^2 chart when the shifts are small ($\delta_{opt} \leq 1.00$) for both zero-state and steady-state cases since the *QDRL*s of the VSS MEWMA chart are smaller than that of the standard MEWMA chart and the synthetic T^2 chart. For example, at $\delta_{opt} = 0.25$ for $p = 2$, the zero-state *QDRL*s for the VSS MEWMA chart, the standard MEWMA chart and the synthetic T^2 chart are 8.5, 13.5 and 123.5, respectively. However, the difference in the *QDRL* is not significant between the control charts at the larger shifts ($\delta_{opt} \geq 1.50$). The

results for the VSS MEWMA chart and the standard MEWMA chart are verified via Monte Carlo simulation.

8. Illustrative Example

An example is presented in this section to illustrate the implementation of a VSS MEWMA chart based on the steady-state *MRL*. The implementation of the corresponding standard MEWMA chart is also discussed for the sake of comparison. The monitoring process is the operation of an aluminium smelter with the known in-control process mean vector is $\tilde{\boldsymbol{\mu}}_0 = (-0.1083, 0.0162, 0.0573, -0.0085, 1.0893)^T$ and the known process covariance matrix is

$$\tilde{\boldsymbol{\Sigma}} = \begin{pmatrix} 0.1727 & 0.0628 & -0.0276 & -0.0127 & -0.0033 \\ 0.0628 & 0.3307 & -0.3019 & -0.0167 & 0.0332 \\ -0.0276 & -0.3019 & 0.5313 & -0.0602 & -0.0007 \\ -0.0127 & -0.0167 & -0.0602 & 0.1897 & -0.0240 \\ -0.0033 & 0.0332 & -0.0007 & -0.0240 & 0.0336 \end{pmatrix},$$

taken from Nishimura, Matsuura, and Suzuki (2015).

The first 200 observations are generated from a multivariate normal distribution with the given $\tilde{\boldsymbol{\mu}}_0$ and $\tilde{\boldsymbol{\Sigma}}$. After that, the remaining observations are generated using the distribution with the same $\tilde{\boldsymbol{\Sigma}}$ but the process starts to shift with the process mean vector, $\tilde{\boldsymbol{\mu}}_1 = (-0.1865, 0.0183, 0.0928, -0.0454, 1.0878)^T$. These observations are plotted on the VSS MEWMA chart and the standard MEWMA chart in Figures 2 and 3, respectively. The generated data for both charts can be accessed at https://www.researchgate.net/publication/310597075_Supplementary_Materials_for_VSS_MEWMA?ev=prf_pub (Tables S1 and S2 in supplementary material).

It is assumed that δ_{opt} = 0.25 is the most distinct variation in the process mean vector to be detected quickly during the process monitoring. The VSS MEWMA chart and the standard MEWMA chart are optimized at δ_{opt} = 0.25 with MRL_0 = 350, p = 5 and $E(n)$ = 5. The optimal charting parameters for the VSS MEWMA chart are (r, n_1, n_2, H, w) = (0.10, 2, 18, 17.153, 7.228) and the optimal charting parameters for the standard MEWMA chart are (r, H) = (0.05, 15.827) (see Table 2).

The concept of the VSS MEWMA chart is that the next sample would be the small sample of size n_1 = 2 if the current plotted chart statistic falls inside the safety region ($T_t^2 \le w$). On the other hand, the next sample would be the large sample of size n_2 = 18 if the current plotted chart statistic falls inside the warning region ($w < T_t^2 \le H$). The sampling scheme for this VSS MEWMA chart is defined by the following function:

$$n = \begin{cases} 2 & \text{if } T_t^2 \le 7.228 \\ 18 & \text{if } 7.228 < T_t^2 \le 17.153 \end{cases}.$$

In Figure 2, the symbols ♦ and ▲ represent the small sample of size n_1 and the large sample of size n_2, respectively. The VSS MEWMA chart is implemented as follows: The sample mean vector at the first sampling point (t = 1) obtained using n_2 = 18 is computed as $\overline{\mathbf{X}}_1$ = (–0.0015, 0.0715, 0.0465, 0.0342, 1.0385)^T using Equation (1) and the corresponding standardized sample mean vector is calculated as $\tilde{\mathbf{Z}}_1$ = (1.0907, 0.4080, –0.0631, 0.4155, –1.1761)^T using Equation (2). The in-control process standard deviation vector is obtained as the square root of the elements of $\tilde{\boldsymbol{\Sigma}}$ on the main diagonal and is calculated as $\tilde{\boldsymbol{\sigma}}_0$ = ($\sqrt{0.1727}$, $\sqrt{0.3307}$, $\sqrt{0.5313}$, $\sqrt{0.1897}$,

$\sqrt{0.0336}$)^T = (0.4156, 0.5750, 0.7289, 0.4356, 0.1834)^T. Then, the MEWMA vector is calculated as $\tilde{\mathbf{W}}_1$ = (0.1091, 0.0408, –0.0063, 0.0415, –0.1176)^T using Equation (3) and the corresponding plotted chart statistic is calculated as T_1^2 = 0.63 using Equation (4). Since this chart statistic falls inside the safety region, then the small sample of size n_1 = 2 will be used for the next sampling point. This process is continued until the 86th sampling point (t = 86) with the plotted chart statistic calculated as T_{86}^2 = 8.23. This sample falls inside the warning region, then the large sample of size n_2 = 18 will be used for the next sampling point (t = 87). This process then is continued until the 231st sampling point (t = 231), where this VSS MEWMA chart detects the out-of-control signal at this sampling point since (T_{231}^2 = 17.73) > H, where H = 17.153.

The standard MEWMA chart is implemented as follows (see Figure 3): At the 1st sampling point, the sample mean vector with a fixed sample of size n_0 = 5 is computed as $\overline{\mathbf{X}}_1$ = (–0.0209, –0.0899, –0.3193, 0.3410, 0.9827)^T using Equation (1) and the corresponding standardized sample mean vector is calculated as $\tilde{\mathbf{Z}}_1$ = (0.4702, –0.4126, –1.1553, 1.7941, –1.2997)^T using Equation (2). Then, the MEWMA vector at this sampling point is calculated as $\tilde{\mathbf{W}}_1$ = (0.0235, –0.0206, –0.0578, 0.0897, –0.0650)^T using Equation (3) and the corresponding plotted chart statistic is calculated as T_1^2 = 0.65 using Equation (4). This process is continued until the out-of-control signal is detected at the 247th sampling point (t = 247) since (T_{247}^2 = 16.74) > H, where H = 15.827.

The comparison between the standard MEWMA chart and the VSS MEWMA chart highlights that the latter is quicker in detecting the out-of-control signal compared to the former. In other words, the VSS MEWMA chart detects the out-of-control signal

at a much earlier time than the standard MEWMA chart. This result clearly demonstrates the superiority of the VSS MEWMA chart over the standard MEWMA chart in detecting shifts in the process mean vector. The VSS MEWMA chart has a steady-state MRL_1 of 21 in detecting δ_{opt} = 0.25. In comparison, the corresponding standard MEWMA chart has a steady-state MRL_1 of 31 (see Table 3). The MRL_1 value of the standard MEWMA chart is about $(31 - 21)/31 \times 100 = 32\%$ more than that of the VSS MEWMA chart.

9. Conclusions

This paper presents the optimal statistical design of the VSS MEWMA chart based on the *MRL*. The shape of the run-length probability distribution for the VSS MEWMA chart changes with the shift in the process mean vector, ranging from being highly right skewed when the process is in control to being almost symmetric when the shift is large. Thus, the *MRL* is proposed as a performance measure for the VSS MEWMA chart, instead of the *ARL* for ease of interpretation. The percentage points of the run-length for the different magnitude of shifts in the process mean vector are also included for a better understanding of the VSS MEWMA chart.

From the numerical comparison, it is noticeable that the MRL_1 and the *QDRL* of the VSS MEWMA chart are smaller than that of the standard MEWMA chart and the synthetic T^2 chart. This means that the VSS MEWMA chart performs better than the standard MEWMA chart and the synthetic T^2 chart for detecting shifts in the process mean vector.

References

Aly, A.A., Mahmoud, M.A., & Hamed, R. (2016). The performance of the multivariate adaptive exponentially weighted moving average control chart with estimated

parameters. *Quality and Reliability Engineering International, 32*, 957–967. doi: 10.1002/qre.1806
Aparisi, F. (1996). Hotelling's T^2 control chart with adaptive sample sizes. *International Journal of Production Research, 34*, 2853–2862. doi: 10.1080/00207549608905062
Aparisi, F., Epprecht, E., Carrión, A., & Ruiz, O. (2014). The variable sample size variable dimension T^2 control chart. *International Journal of Production Research, 52*, 368–383. doi: 10.1080/00207543.2013.826832
Bersimis, S., Psarakis, S. and Panaretos, J. (2007). Multivariate statistical process control charts: an overview. *Quality and Reliability Engineering International*, *23*, 517–543. doi: 10.1002/qre.829
Brook, D., & Evans, D.A. (1972). An approach to the probability distribution of cusum run length. *Biometrika*, *59*, 539–549. doi: 10.1093/biomet/59.3.539
Castagliola, P., Achouri, A., Taleb, H., Celano, G., & Psarakis, S. (2015). Monitoring the coefficient of variation using a variable sample size control chart. *The International Journal of Advanced Manufacturing Technology, 80*, 1561–1576. doi: 10.1007/s00170-015-6985-6
Castagliola, P., Zhang, Y., Costa, A., & Maravelakis, P. (2012). The variable sample size $\overline{X}$ chart with estimated parameters. *Quality and Reliability Engineering International, 28*, 687–699. doi: 10.1002/qre.1261
Chakraborti, S. (2007). Run length distribution and percentiles: the Shewhart chart with unknown parameters. *Quality Engineering, 19*, 119–127. doi: 10.1080/08982110701276653
Champ, C.W. (1992). Steady-state run length analysis of a Shewhart quality control chart with supplementary runs rules. *Communications in Statistics – Theory and Methods, 21*, 765–777. doi: 10.1080/03610929208830813
Chen, N., Zi, X., & Zou, C. (2016). A distribution-free multivariate control chart. *Technometrics*, *58*, 448–459. doi: 10.1080/00401706.2015.1049750
Cheng, S.W., & Mao, H. (2011). The economic design of multivariate MSE control chart. *Quality Technology & Quantitative Management, 8*, 75–85. doi: 10.1080/16843703.2011.11673248
Chin, W.S., & Khoo, M.B.C. (2012). A study of the median run length (*MRL*) performance of the EWMA *t* chart for the mean. *South African Journal of Industrial Engineering, 23*, 42–55. Retrieved from http://www.scielo.org.za/pdf/sajie/v23n3/06.pdf
Das, N. (2009). A new multivariate non-parametric control chart based on sign test. *Quality Technology & Quantitative Management, 6*, 155–169. doi: 10.1080/16843703.2009.11673191
Dyer, J.N., Adams, B.M., & Conerly, M.D. (2003). The reverse moving average control chart for monitoring autocorrelated processes. *Journal of Quality Technology, 35*, 139–152. Retrieved from http://asq.org/data/subscriptions/jqt_open/2003/april/qtec-35-2-139.html
Faraz, A., & Moghadam, M.B. (2009). Hotelling's T^2 control chart with two adaptive sample sizes. *Quality & Quantity, 43*, 903–912. doi: 10.1007/s11135-008-9167-x
Gan, F.F. (1993). An optimal design of ewma control charts based on median run length. *Journal of Statistical Computation and Simulation, 4*, 169–184. doi: 10.1080/00949659308811479
Ghute, V.B., & Shirke, D.T. (2008a). A multivariate synthetic control chart for monitoring process mean vector. *Communications in Statistics – Theory and Methods, 37*, 2136–2148. doi: 10.1080/03610920701824265

Ghute, V.B., & Shirke, D.T. (2008b). A multivariate synthetic control chart for process dispersion. *Quality Technology & Quantitative Management, 5*, 271–288. doi: 10.1080/16843703.2008.11673401
Golosnoy, V., & Schmid, W. (2007). EWMA control charts for monitoring optimal portfolio weights. *Sequential Analysis, 26*, 195–224. doi: 10.1080/07474940701247099
Graham, M.A., Chakraborti, S., & Mukherjee, A. (2014). Design and implementation of CUSUM exceedance control charts for unknown location. *International Journal of Production Research, 52*, 5546–5564. doi: 10.1080/00207543.2014.917214
Graham, M.A., Mukherjee, A., & Chakraborti, S. (2012). Distribution-free exponentially weighted moving average control charts for monitoring unknown location. *Computational Statistics & Data Analysis, 56*, 2539–2561. doi: 10.1016/j.csda.2012.02.010
Haq, A., & Khoo, M.B.C. (2016). A new synthetic control chart for monitoring process mean using auxiliary information. *Journal of Statistical Computation and Simulation, 86*, 3068–3092. doi: 10.1080/00949655.2016.1150477
Huang, W., Shu, L., Woodall, W.H., & Tsui, K.L. (2016). CUSUM procedures with probability control limits for monitoring processes with variable sample sizes. *IIE Transactions, 48*, 759–771. doi: 10.1080/0740817X.2016.1146422
Khoo, M.B.C., Teh, S.Y., Chuah, S.K., & Foo, T.F. (2011). A comparison on the *MRL* performances of optimal MEWMA and optimal MCUSUM control charts. *International Journal on Advanced Science, Engineering and Information Technology, 1*, 31–35. doi: 10.18517/ijaseit.1.1.9
Khoo, M.B.C., Wong, V.H., Wu, Z., & Castagliola, P. (2011). Optimal designs of the multivariate synthetic chart for monitoring the process mean vector based on median run length. *Quality and Reliability Engineering International, 27*, 981–997. doi: 10.1002/qre.1189
Khoo, M.B.C., Wong, V.H., Wu, Z., & Castagliola, P. (2012). Optimal design of the synthetic chart for the process mean based on median run length. *IIE Transactions, 44*, 765–779. doi: 10.1080/0740817X.2011.609526
Kooli, I., & Limam, M. (2011). Economic design of an attribute *np* control chart using a variable sample size. *Sequential Analysis, 30*, 145–159. doi: 10.1080/07474946.2011.563703
Lee, M.H. (2010). Multivariate EWMA control chart with adaptive sample sizes. *Communications in Statistics – Simulation and Computation, 39*, 1548–1561. doi:10.1080/03610918.2010.507897
Lee, M.H. (2013). Variable sampling rate multivariate exponentially weighted moving average control chart with double warning lines. *Quality Technology & Quantitative Management, 10*, 353–368. doi: 10.1080/16843703.2013.11673420
Lee, M.H., & Khoo, M.B.C. (2006). Optimal statistical design of a multivariate EWMA chart based on *ARL* and *MRL*. *Communications in Statistics – Simulation and Computation, 35*, 831–847. doi: 10.1080/03610910600716779
Li, J., Tsung, F., & Zou, C. (2014). Multivariate binomial/multinomial control chart. *IIE Transactions, 46*, 526–542. doi: 10.1080/0740817X.2013.849830
Low, C.K., Khoo, M.B.C., Teoh, W.L., & Wu, Z. (2012). The revised m-of-k runs rule based on median run length. *Communications in Statistics – Simulation and Computation, 41*, 1463–1477. doi: 10.1080/03610918.2011.606950
Lowry, C.A., & Montgomery, D.C. (1995). A review of multivariate control charts. *IIE Transactions, 27*, 800–810. doi: 10.1080/07408179508936797

Lowry, C.A., Woodall, W.H., Champ, C.W., & Rigdon, S.E. (1992). A multivariate exponentially weighted moving average control chart. *Technometrics, 34*, 46–53. doi: 10.1080/00401706.1992.10485232
Maboudou-Tchao, E.M., & Diawara, N. (2013). A lasso chart for monitoring the covariance matrix. *Quality Technology & Quantitative Management, 10*, 95–114. doi: 10.1080/16843703.2013.11673310
Mahmoud, M.A., & Maravelakis, P.E. (2010). The performance of the MEWMA control chart when parameters are estimated. *Communications in Statistics – Simulation and Computation, 39*, 1803–1817. doi: 10.1080/03610918.2010.518269
Mahmoud, M.A., & Zahran, A.R. (2010). A multivariate adaptive exponentially weighted moving average control chart. *Communications in Statistics – Theory and Methods, 39*, 606–625. doi: 10.1080/03610920902755813
Maravelakis, P.E., Panaretos, J., & Psarakis, S. (2005). An examination of the robustness to non normality of the EWMA control charts for the dispersion. *Communications in Statistics – Simulation and Computation, 34*, 1069–1079. doi: 10.1080/03610910500308719
Molnau, W., Runger, G., Montgomery, D., Skinner, K., Loredo, E., & Prabhu, S. (2001). A program for *ARL* calculation for multivariate EWMA charts. *Journal of Quality Technology, 33*, 515–521. Retrieved from http://search.proquest.com/openview/cc9538e7454a739e046d7e9decd8213d/1?pq-origsite=gscholar
Montgomery, D.C. (2013). *Introduction to statistical quality control* (7th ed.). New York, NY: John Wiley & Sons.
Mukherjee, A., & Marozzi, M. (2016a). A distribution-free phase-II CUSUM procedure for monitoring service quality. *Total Quality Management & Business Excellence*. Advance online publication. doi: 10.1080/14783363.2015.1134266
Mukherjee, A., & Marozzi, M. (2016b). Distribution-free lepage type circular-grid charts for joint monitoring of location and scale parameters of a process, *Quality and Reliability Engineering International*. Advance online publication. doi: 10.1002/qre.2002
Nishimura, K., Matsuura, S., & Suzuki, H. (2015). Multivariate EWMA control chart based on a variable selection using AIC for multivariate statistical process monitoring. *Statistics & Probability Letters, 104*, 7–13. doi: 10.1016/j.spl.2015.05.003
Palm, A.C. (1990). Tables of run length percentiles for determining the sensitivity of Shewhart control charts for averages with supplementary runs rules. *Journal of Quality Technology, 22*, 289–298. Retrieved from http://asq.org/qic/display-item/index.pl?item=11273
Park, J., & Jun, C.H. (2015). A new multivariate EWMA control chart via multiple testing. *Journal of Process Control, 26*, 51–55. doi: 10.1016/j.jprocont.2015.01.007
Prabhu, S.S., Runger, G.C., & Montgomery, D.C. (1997). Selection of the subgroup size and sampling interval for a CUSUM control chart. *IIE Transactions, 29*, 451–457. doi: 10.1023/a:1018516506199
Qiu, P. (2013). *Introduction to statistical process control*. Boca Raton, FL: Chapman & Hall/CRC Press.
Reynolds Jr., M.R., & Cho, G.Y. (2011). Multivariate control charts for monitoring the mean vector and covariance matrix with variable sampling intervals. *Sequential Analysis, 30*, 1–40. doi: 10.1080/07474946.2010.520627
Runger, G.C., & Prabhu, S.S. (1996). A markov chain model for the multivariate exponentially weighted moving averages control chart. *Journal of the American Statistical Association, 91*, 1701–1706. doi: 10.1080/01621459.1996.10476741

Seif, A., Faraz, A., & Sadeghifar, M. (2015). Evaluation of the economic statistical design of the multivariate T^2 control chart with multiple variable sampling intervals scheme: NSGA-II approach. *Journal of Statistical Computation and Simulation, 85*, 2442–2455. doi: 10.1023/A:1018516506199

Shen, X., Tsung, F., & Zou, C. (2014). A new multivariate EWMA scheme for monitoring covariance matrices. *International Journal of Production Research, 52*, 2834–2850. doi: 10.1080/00207543.2013.842019

Stoumbos, Z.G., Mittenthal, J., & Runger, G.C. (2001). Steady-state-optimal adaptive control charts based on variable sampling intervals. *Stochastic Analysis and Applications, 19*, 1025–1057. doi: 10.1081/SAP-120000759

Teoh, W.L., Khoo, M.B.C., & Teh, S.Y. (2013). Optimal designs of the median run length based double sampling $\bar{X}$ chart for minimizing the average sample size. *PLoS ONE, 8*(7), 1–11. doi: 10.1371/journal.pone.0068580

Zi, X., Zou, C., Zhou, Q., & Wang, J. (2013). A directional multivariate sign EWMA control chart. *Quality Technology & Quantitative Management, 10*, 115–132. doi: 10.1080/16843703.2013.11673311

Zou, C., & Tsung, F. (2011). A multivariate sign EWMA control chart. *Technometrics, 53*, 84–97. doi: 10.1198/TECH.2010.09095

Table 1. Percentage points of the run-length for the steady-state VSS MEWMA chart ($p = 2$, $E(n) = 5$ and $ARL_0 \approx 500$).

Optimal charting parameters	δ	*ARL*	Percentage points										
			1st	5th	10th	20th	30th	40th	50th	60th	70th	80th	90th
$\delta_{opt} = 0.50$	0.00	498.33	5	26	53	112	178	255	346	457	600	802	1147
	0.25	32.61	2	4	6	10	14	18	24	30	39	51	71
	0.50	7.15	1	2	2	3	4	5	6	7	8	10	14
$(r, n_1, n_2, H, w) = (0.43, 1, 21, 12.228, 3.197)$	1.00	3.44	1	1	1	2	2	2	3	3	4	5	6
	1.50	2.59	1	1	1	1	2	2	2	3	3	4	4
	2.00	2.19	1	1	1	1	2	2	2	2	3	3	3
$\delta_{opt} = 1.00$	0.00	499.20	6	26	53	112	178	255	346	462	601	803	1149
	0.25	86.10	2	6	11	21	32	45	60	79	103	138	196
	0.50	11.28	1	2	3	4	6	7	9	11	13	17	23
$(r, n_1, n_2, H, w) = (0.61, 1, 10, 12.343, 1.613)$	1.00	2.73	1	1	1	2	2	2	2	3	3	4	5
	1.50	1.85	1	1	1	1	1	2	2	2	2	2	3
	2.00	1.62	1	1	1	1	1	1	2	2	2	2	2

Table 2. Zero-state and steady-state optimal charting parameters for the VSS MEWMA chart, the standard MEWMA chart and the synthetic T^2 chart ($E(n) = 5$ and $MRL_0 = 350$).

δ_{opt}	p	Zero-state			Steady-state		
		VSS MEWMA	standard MEWMA	synthetic T^2	VSS MEWMA	standard MEWMA	synthetic T^2
		$(r,\ n_1,\ n_2, H, w)$	(r, H)	(L, CL)	$(r,\ n_1,\ n_2, H, w)$	(r, H)	(L, CL)
0.25	2	(0.19, 3, 20, 11.615, 4.150)	(0.11, 10.929)	(67, 10.4541)	(0.10, 4, 12, 10.790, 1.360)	(0.10, 10.790)	(4, 7.6203)
	3	(0.17, 2, 20, 13.855, 4.96)	(0.05, 11.903)	(86, 12.961)	(0.10, 4, 14, 13.124, 2.281)	(0.05, 11.903)	(3, 9.3007)
	5	(0.11, 3, 16, 17.310, 7.780)	(0.05, 15.827)	(91, 16.9552)	(0.10, 2, 18, 17.153, 7.228)	(0.05, 15.827)	(3, 12.7782)
0.50	2	(0.35, 3, 15, 12.131, 3.601)	(0.16, 11.419)	(11, 8.6291)	(0.34, 1, 12, 12.115, 1.975)	(0.19, 11.614)	(6, 8.0241)
	3	(0.30, 4, 13, 14.401, 5.869)	(0.18, 13.920)	(16, 11.1219)	(0.35, 2, 16, 14.510, 4.450)	(0.19, 13.979)	(5, 9.8575)
	5	(0.30, 3, 14, 18.499, 7.426)	(0.17, 17.928)	(24, 15.3300)	(0.31, 1, 17, 18.525, 6.570)	(0.15, 17.766)	(6, 13.6357)
1.00	2	(0.50, 3, 6, 12.305, 0.776)	(0.50, 12.305)	(2, 6.9318)	(0.62, 1, 9, 12.365, 1.380)	(0.43, 12.245)	(1, 6.2456)
	3	(0.47, 3, 6, 14.655, 1.530)	(0.43, 14.615)	(2, 8.8577)	(0.70, 1, 12, 14.749, 3.267)	(0.40, 14.580)	(3, 9.3007)
	5	(0.48, 4, 7, 18.760, 5.75)	(0.40, 18.680)	(3, 12.7782)	(0.48, 1, 6, 18.760, 2.360)	(0.30, 18.499)	(3, 12.7782)
1.50	2	(0.62, 2, 6, 12.365, 0.520)	(0.30, 12.030)	(1, 6.2456)	(0.98, 1, 6, 12.403, 0.476)	(0.60, 12.355)	(1, 6.2456)
	3	(0.65, 2, 6, 14.738, 1.178)	(0.60, 14.723)	(1, 8.0978)	(0.58, 1, 6, 14.720, 1.017)	(0.59, 14.720)	(1, 8.0978)
	5	(0.65, 2, 6, 18.834, 2.607)	(0.63, 18.829)	(1, 11.3981)	(0.60, 1, 6, 18.820, 2.345)	(0.62, 18.826)	(1, 11.3981)
2.00	2	(0.90, 3, 6, 12.402, 0.781)	(0.70, 12.385)	(1, 6.2456)	(0.65, 1, 6, 12.375, 0.455)	(0.70, 12.385)	(1, 6.2456)
	3	(0.80, 4, 6, 14.762, 2.361)	(0.70, 14.749)	(1, 8.0978)	(0.70, 1, 6, 14.749, 1.020)	(0.70, 14.749)	(1, 8.0978)
	5	(0.89, 4, 6, 18.862, 4.294)	(0.80, 18.857)	(1, 11.3981)	(0.74, 1, 6, 18.853, 2.349)	(0.70, 18.845)	(1, 11.3981)
2.50	2	(0.87, 2, 6, 12.400, 0.554)	(0.65, 12.370)	(1, 6.2456)	(0.60, 1, 6, 12.355, 0.411)	(0.60, 12.355)	(1, 6.2456)
	3	(0.74, 3, 6, 14.755, 1.543)	(0.60, 14.723)	(1, 8.0978)	(0.60, 1, 6, 14.723, 1.018)	(0.60, 14.723)	(1, 8.0978)
	5	(0.80, 3, 6, 18.857, 3.161)	(0.65, 18.834)	(1, 11.3981)	(0.63, 1, 6, 18.833,2.346)	(0.70, 18.845)	(1, 11.3981)

Table 3. Zero-state and steady-state MRL_1s of the VSS MEWMA chart, standard MEWMA chart and the synthetic T^2 chart ($E(n) = 5$ and $MRL_0 = 350$).

δ_{opt}	p	Zero-state					Steady-state				
		VSS MEWMA		standard MEWMA		synthetic T^2	VSS MEWMA		standard MEWMA		synthetic T^2
		Markov chain approach	Monte Carlo simulation	Markov chain approach	Monte Carlo simulation		Markov chain approach	Monte Carlo simulation	Markov chain approach	Monte Carlo simulation	
0.25	2	17	17	21	26	67	15	15	25	25	157
	3	20	20	29	29	86	15	15	28	28	187
	5	24	24	33	34	151	21	21	31	32	223
0.50	2	6	5	7	9	11	6	6	9	9	31
	3	7	6	10	10	16	6	6	10	10	43
	5	8	7	12	12	24	7	7	11	11	63
1.00	2	3	3	3	3	2	2	2	3	3	4
	3	3	3	3	3	2	3	3	3	3	4
	5	3	3	4	4	3	3	3	3	4	6
1.50	2	2	1	2	2	1	1	2	2	2	2
	3	2	2	2	2	1	2	2	2	2	2
	5	2	2	2	2	1	2	2	2	2	2
2.00	2	1	1	1	1	1	1	1	1	1	2
	3	1	1	1	1	1	1	1	1	1	2
	5	1	1	1	1	1	1	1	1	1	2
2.50	2	1	1	1	1	1	1	1	1	1	2
	3	1	1	1	1	1	1	1	1	1	2
	5	1	1	1	1	1	1	1	1	1	2

Table 4. Zero-state and steady-state *QDRL*s of the VSS MEWMA chart, the standard MEWMA chart and the synthetic T^2 chart ($E(n) = 5$ and $MRL_0 = 350$).

δ_{opt}	p	Zero-state					Steady-state				
		VSS MEWMA		standard MEWMA		synthetic T^2	VSS MEWMA		standard MEWMA		synthetic T^2
		Markov chain approach	Monte Carlo simulation	Markov chain approach	Monte Carlo simulation		Markov chain approach	Monte Carlo simulation	Markov chain approach	Monte Carlo simulation	
0.25	2	8.5	9.0	13.5	13.5	123.5	5.5	5.5	13.0	12.5	124.0
	3	9.5	11.0	10.5	10.0	157.5	5.5	5.5	11.0	11.0	148.5
	5	9.5	10.0	12.0	12.0	202.0	10.0	10.0	12.5	12.5	176.0
0.50	2	2.0	2.0	3.0	3.0	20.0	2.5	2.5	3.5	3.5	24.5
	3	2.5	3.0	3.5	3.5	28.0	2.5	2.5	3.5	3.5	34.0
	5	3.0	3.0	4.5	4.5	43.5	3.0	3.0	4.0	4.0	50.0
1.00	2	1.0	1.0	1.0	1.0	1.5	0.5	0.5	1.0	1.0	2.5
	3	1.0	1.0	1.0	1.0	2.5	1.0	1.0	1.5	1.5	3.0
	5	1.0	1.0	1.0	1.0	3.5	1.5	1.5	1.0	1.0	4.5
1.50	2	0.0	0.5	0.0	0.0	0.0	0.5	0.5	0.5	0.5	0.5
	3	0.5	0.5	0.5	0.5	0.0	0.5	0.5	0.5	0.5	1.0
	5	0.5	0.5	1.0	0.5	0.5	0.5	0.5	0.5	0.5	1.5
2.00	2	0.5	0.0	0.0	0.0	0.0	0.5	0.5	0.0	0.0	0.5
	3	0.5	0.0	0.5	0.0	0.0	0.5	0.5	0.5	0.5	0.5
	5	0.5	0.0	0.5	0.5	0.0	0.5	0.5	0.5	0.5	0.5
2.50	2	0.5	0.0	0.5	0.0	0.0	0.0	0.0	0.0	0.0	0.5
	3	0.5	0.0	0.0	0.0	0.0	0.0	0.0	0.0	0.0	0.5
	5	0.5	0.0	0.0	0.0	0.0	0.0	0.0	0.0	0.0	0.5

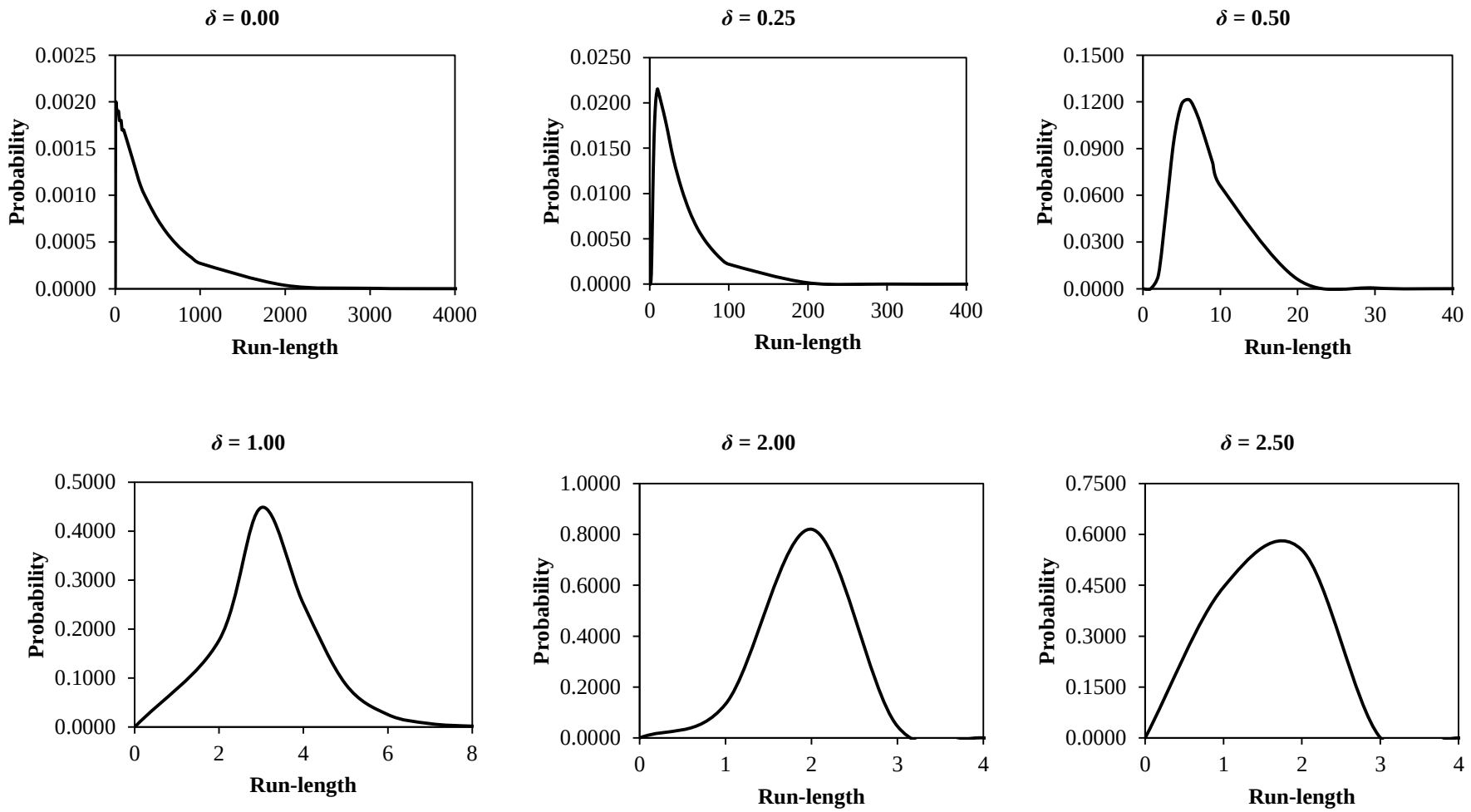

Figure 1. Plots of the run-length probability distribution for the zero-state VSS MEWMA chart ($E(n) = 5$, $MRL_0 = 350$, $p = 3$ and $\delta_{opt} = 0.50$).

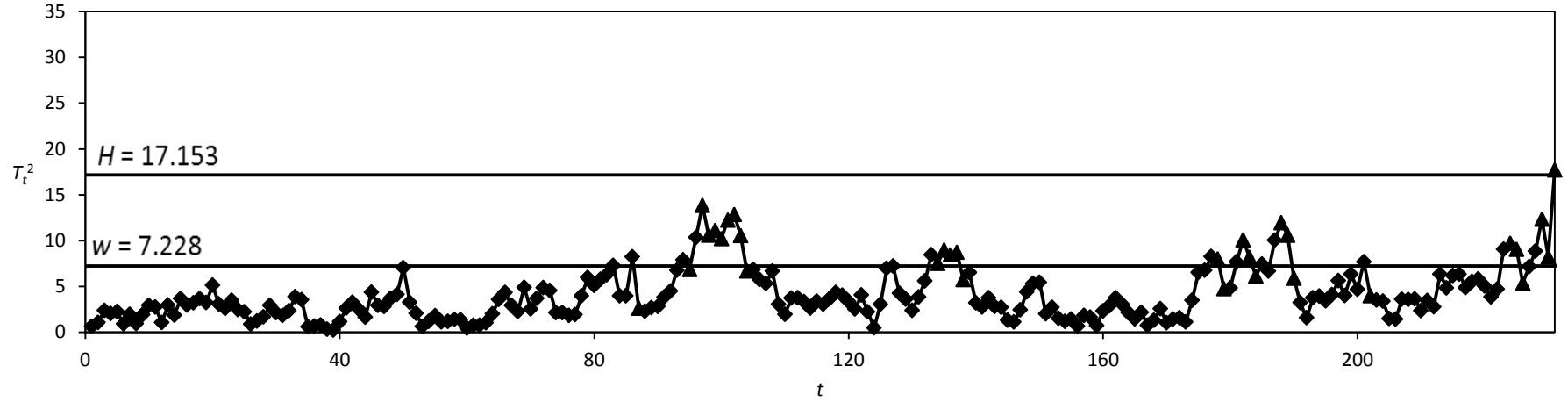

Figure 2. The VSS MEWMA chart for the illustrative example.

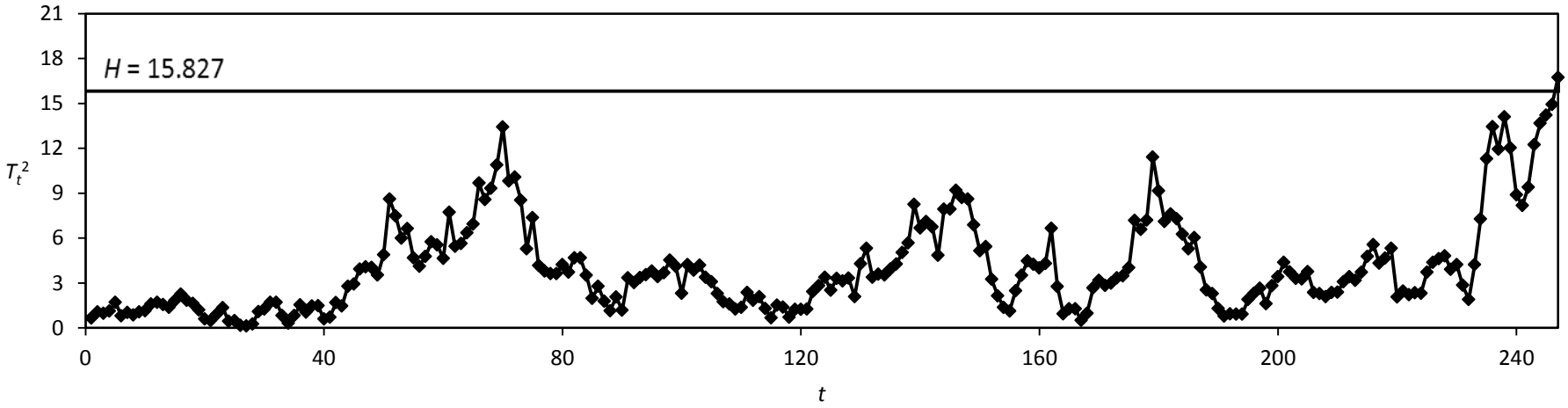

Figure 3. The standard MEWMA chart for the illustrative example.